# High-Speed Back Emitting VCSEL with HCG Meta Lens

Yao Cui (1,2,4), Yipeng Ji (1,4), Binbin Zhao (1), Shasha Li (1), Zhenglai Zhang (1), Jonas Kapraun (1), Huawen Hu (1), Jiaxing Wang (1), ChihChiang Shen (1), Connie J. Chang-Hasnain (1,2,3)

- (1) Berxel Photonics Co. Ltd., Shenzhen 518071, China, connie.chang@berxel.com
- (2) Tsinghua-Berkeley Shenzhen Institute, Tsinghua University, Shenzhen 518055, China
- (3) School of Science and Engineering, the Chinese University of Hong Kong, Shenzhen, 518172, China
- (4) These authors contributed equally: Yao Cui, Yipeng Ji

**Abstract** We integrate a high-contrast-grating metalens on a 940-nm flip-chip back-emitting VCSEL, which results in a greatly reduced beam divergence to <6 degrees with a built-in anti-reflection. The device exhibits error-free 25 Gb/s transmission over 100 m OM4 fiber and 15 GHz S21-3dB bandwidth. ©2025 The Author(s)

### Introduction

Recently, generative AI applications have created a massive drive on the demands for computational power. The resulting scaling up of Graphics Processing Unit (GPU) clusters faces challenges in bandwidth density and reach. High speed parallel optical interconnects are promising for the fast-growing bandwidth demands in the era of accelerated Al workloads and data-intensive applications. Flip-chip packaged backemitting vertical-cavity surface-emitting laser (VCSEL) are promising to realize ultrahigh aggregate bandwidth density with the potential to create an array with hundreds of 10~100Gbps emitters with link energy well under 1 pJ/bit. Nevertheless, one of the most challenging and communal problems for optical interconnects is the lack of cost-effective optical coupling scheme from laser/waveguide arrays to optical fiber arrays.

In this work, we present a novel 940 nm backemitting, high-speed VCSEL array with monolithically integrated high-contrast grating (HCG) meta lens on the substrate side of each VCSEL. The HCG meta lens is a flat optics with nearwavelength metastructures to create an optical phase front of a lens. Here, the HCG was designed to function not only to provide collimation but also anti-reflection. We show significantly reduced VCSEL beam divergence, which increased optical coupling efficiency to as-cleaved multimode optical fibers. We report a novel frontback alignment fabrication technique leveraging the architecture of a flat lens, which enables precise alignment of VCSEL center (on the front side) to lens center (back substrate). This alignment accuracy and control is shown to be important for reduced RIN noise and higher optical coupling efficiency. The VCSELs exhibit error-free 25 Gb/s transmission over 100 m OM4 fiber and 15 GHz S21-3dB bandwidth.

## Process of VCSEL and HCG meta lens

The back emitting VCSEL is fabricated on the front side of a 940nm GaAs based epitaxial wafer optimized for backside emission, schematically shown in Fig. 1(a). Plated Gold N- and P-contact pads of the VCSEL are levelled and define the highest points on the top surface of the wafer to facilitate flip chip bonding onto a chip-on-carrier, shown in Fig. 1(b). Fig. 1(c) shows the cross-sectional schematic of the VCSEL device.

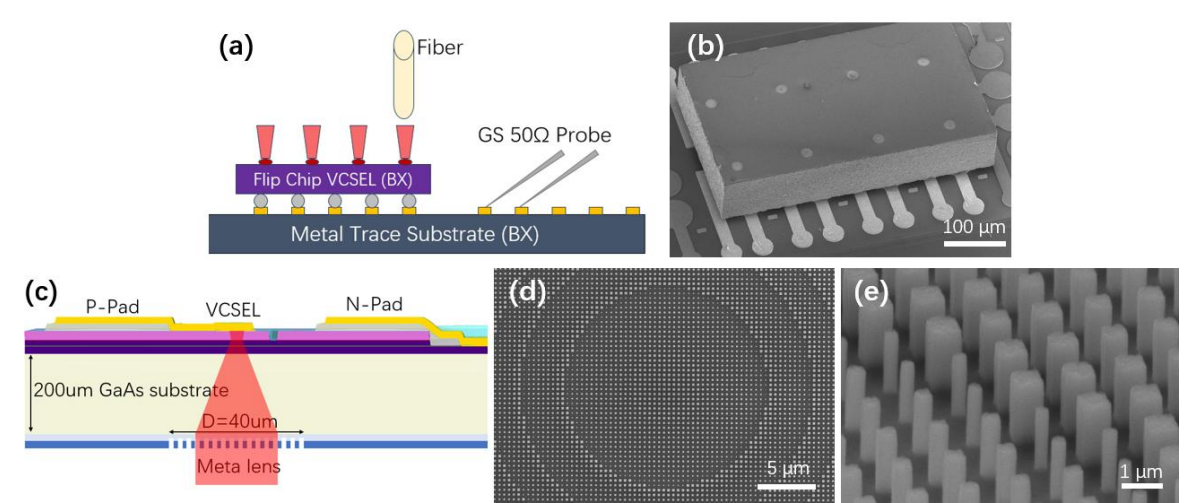


Fig. 1: Flip chip bonded VCSEL with integrated HCG meta lens: (a)schematic of flip chip assembly, (b) tilt view SEM of the same, (c) cross sectional schematic of the VCSEL with integrated HCG meta lens (d) SEM picture of the top view of the HCG metalens (e) high resolution tilt view SEM of the HCG metalens.

After the front side processing steps, the wafer is thinned and polished to 200um thickness. A novel two-step front-back alignment (FBA) technique is used to enable the alignment accuracy of the HCG metalens fabricated on the back side of the substrate. First, a back side alignment key is patterned by a contact mask aligner MA6 with an alignment resolution of 2um followed by metal deposition. Then, Infrared microscope is used to register the front side and back side images simultaneously so that alignment offset can be read. Lastly, the HCG meta lens pattern is defined by electron-beam lithography (EBL) which can compensate alignment offset and dry etch of high index layer. Figure 1(d) shows the top view SEM picture of the HCG meta lens and (e) high resolution tilt view SEM images of the HCG meta lens structure.

The HCG lens consists of a high index contrast layer to be deposited on the polished backside of the substrate. Previous studies show that metasurfaces can be designed to focus, steer, deflect, or control the polarisation of VCSEL beams [1-7], underscoring the value of on-chip flat optics for compact transmitters.

With the 2-step FBA method, the accuracy of HCG Meta lens aligned to VCSEL aperture center is estimated to be better than 0.5um. Some meta lenses are also placed deliberately deviated

from the aperture 5  $\mu$ m in X direction for comparison. After these steps 2x4-element VCSEL arrays are diced and flip chip bonded onto a Silicon substrate with plated gold trace using Ag-paste and a sintering process.

### **Performance of Lensed VCSEL**

Figure 2a shows the light-current (LI) and voltage-current (VI) traces of a back emitting VCSEL with a 200  $\mu$ m substrate and an HCG lens at the back side at room temperature. The LI curve is smooth without ripples and the devices lase with 0.7mA threshold current and have 4.1mW output at 8mA.

Figures 2b–2c confirm spectral integrity: both the chips with/without HCG lens retain the ~940 nm peak with comparable mode structure from 1 mA to 8 mA, confirming that the metasurface does not disturb the cavity. Figure 2d shows 2D far-field patterns (FFP) at the 8mA current. The lens confines the emission to a visibly smaller field-of-view than the bare VCSEL, underscoring its consistent collimation benefit.

Figure 2e presents the angular intensity profiles at 1, 2, 4, and 8 mA. Without the lens (left), the full-width at half-maximum (FWHM) broadens from 5.2° to 14.5° as the current rises, and the curve develops multiple peaks at higher bias. With the HCG lens (right), the FWHM remains within 3.7°–5.5° across the same current range,

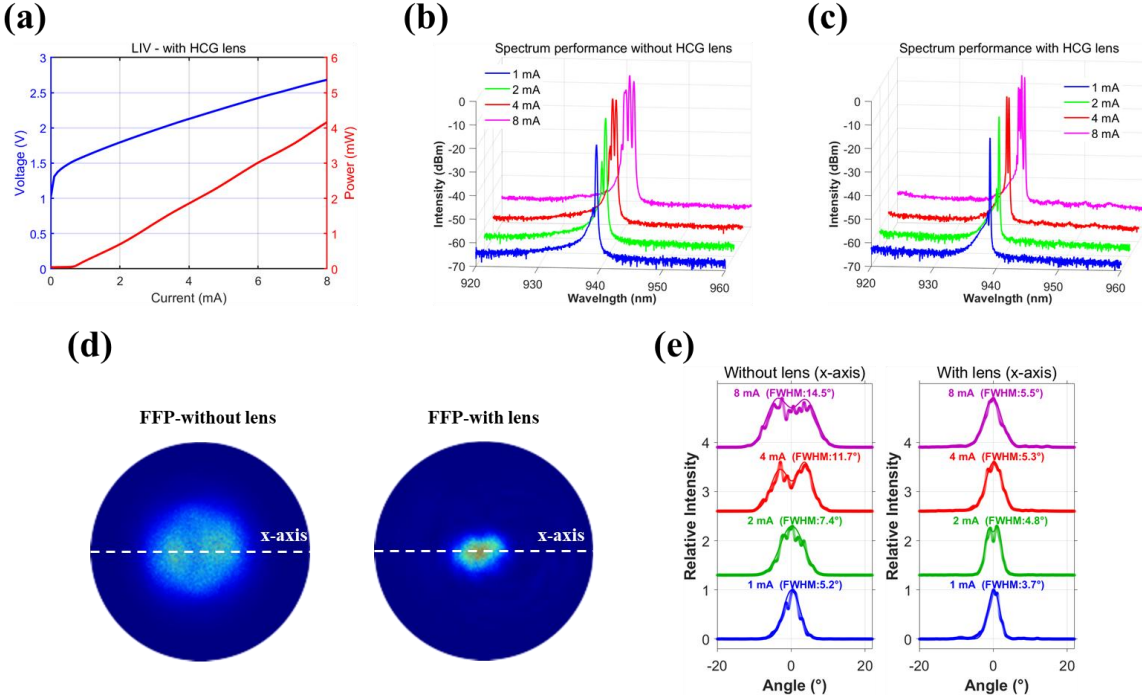


Fig. 2: continuous wave (CW) performance of the flip-chip back-emitting VCSEL without and with the HCG lens. (a) LIV curve of the HCG-lensed VCSEL, it shows the 0.7mA threshold current and has 4.1mW output at 8mA. Spectrum of VCSEL with (b) and without (c) the integrated HCG lens at drive currents of 1, 2, 4 and 8 mA. (d) Far-field images of VCSEL with and without the integrated HCG lens at drive currents of 8mA. (e) One-dimensional far-field of x-axis cuts at 1, 2, 4, 8 mA. Left side shows the VCSEL without HCG lens, the full width at half-maximum (FWHM) widens from 5.2° to 14.5° and multiple peaks appear with increasing current. Right side shows the VCSEL with HCG lens, FWHM stays within 3.7°–5.5° over the same bias range, and the profile remains single-peaked and close to Gaussian.

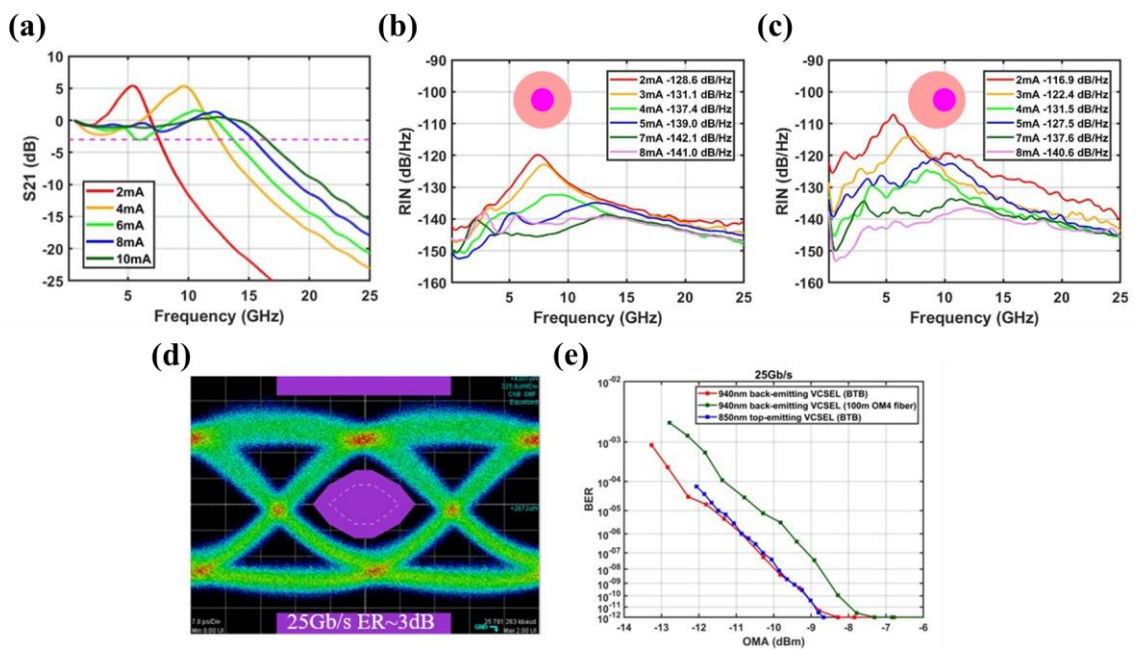


Fig. 3: (a) Small-signal modulation response of the 940 nm back-emitting VCSEL measurement under increasing bias currents. (b) Relative-intensity-noise (RIN) spectra under increasing bias currents, with the HCG lens centred on the oxide aperture. (c) RIN spectra under increasing bias currents with the HCG lens is laterally shifted by 5 μm to the oxide aperture.
(d) Room-temperature eye diagram at 25 Gb/s. (e) Bit error rate versus Optical Modulation Amplitude at 25Gb/s comparison between 940 nm back-emitting and conventional 850 nm top-emitting VCSEL in the indicated link configurations.

and the distribution retains a single, near-Gaussian shape. These data confirm that the metasurface lens keeps the beam narrow and well behaved over the full operating range.

### **High-speed Characteristics**

The VCSEL light was butt-coupled into an ascleaved standard 50/125 µm OM4 multimode fibre, giving a measured coupling efficiency of ~70%. Small-signal modulation response is shown in Fig. 3(a) measured using a 30 GHz photodetector (Thorlabs DXM30AF) and 44 GHz vector network analyzer (Keysight P5027A). The device exhibited a flat frequency response with 3-dB bandwidth of 15 GHz at 8 mA. This 3-dB bandwidth was limited by epitaxy used, which was optimized for high power operation. In the future with optimized epitaxy, we expect much faster high-speed response at lower bias current.

Figures 3(b) and 3(c) show the relative-intensity-noise (RIN) curves. When the HCG lens is centred on the oxide aperture (Fig. 3b), the RIN is lowest; shifting the lens laterally by 5  $\mu$ m (Fig. 3c) increases the mean RIN by 5–7 dB at every drive current, indicating that the lens-to-aperture alignment is critical for low-noise operation.

Figure 3(d) demonstrates the 25 Gb/s NRZ eye diagram measured in compliance with the IEEE 802.3bm standard, achieving a mask margin exceeding 30%. The eye pattern was obtained using an 8 mA DC bias current with an extinction ratio of 3dB. Figure 3(e) shows BER vs. Optical Modulation Amplitude (OMA) measurements at the 25Gbit/s bitrates in the back-to-back

(BTB) and 100m OM4 fiber transmission configurations for 940nm back emitter VCSEL. The PRBS15 and PRBS31 patterns were employed to assess the eye diagram and bit error rate (BER), respectively. The BER performance of 940 nm back-emitting VCSEL is comparable with a conventional 850 nm top-emitting VCSEL.

The 940 nm VCSEL achieved error-free operation (BER < 10<sup>-12</sup>) at OMA of -8.28 dBm (BTB) and -7.30 dBm (100m fiber), showing a 1 dB power penalty attributed to chromatic dispersion. Notably, the sensitivity performance of the proposed back-emitting design matches that of conventional 850 nm top-emitting VCSEL.

#### Conclusions

We demonstrate a back-emitting VCSEL integrated with an HCG meta lens. The meta lens reduces far-field beam divergence by about 2× and delivers smooth, ripple-free power. Direct butt-coupling into as-cleaved standard OM4 multimode fibre already yields a launch efficiency of ~70%. Small-signal tests show a 3-dB bandwidth of 15 GHz at 8 mA under room-temperature operation, and 25 Gb/s links achieve error-free operation over 100 m OM4 fibre with only 1 dB penalty. Because the lens is formed lithographically, no pick-and-place optics are needed, making the device a compact, alignment-tolerant light source for next-generation short-reach interconnects.

### Acknowledgements

This research is supported by the National Key of China under Program Grant 2024YFB2807701, the Shenzhen Science and Technology Program (No. KJZD20240903100208012, No. KQTD20200820113053102, No. ZDSYS20-220325163600001, No. JSGG20220831110404-008, No. KJZ-D20231023100159002), Hetao Shenzhen-Hong Kong science and technology innovation cooperation zone program (No. HZQ-SWSKCCYB202203) and the Guangdong Major Talent Introduction Project (No. 2021ZT09X328)

#### References

- [1] Connie J. Chang-Hasnain, Ye Zhou, Michael C. Y. Huan g, Christopher Chase, "High-contrast grating vertical-cav ity surface-emitting lasers," *IEEE Journal of Selected To pics in Quantum Electronics*, vol. 15, no. 3, pp. 869 – 87 8, 2009, DOI: <a href="https://doi.org/10.1109/JSTQE.2009.2015">https://doi.org/10.1109/JSTQE.2009.2015</a> 195
- [2] Xiangli Jia, Jonas Kapraun, Jiaxing Wang, Jipeng Qi, Yi peng Ji, Connie J. Chang-Hasnain, "Metasurface reflect or enables room-temperature circularly polarized emissi on from VCSEL," Optica, vol. 10, no. 8, pp. 1093 1099, 2023, DOI: <a href="https://doi.org/10.1364/OPTICA.490176">https://doi.org/10.1364/OPTICA.490176</a>
- [3] Yao Cui, Huawen Hu, Yipeng Ji, Jonas Kapraun, Jiaxing Wang, Xuanlun Huang, Connie J. Chang-Hasnain, "Sin gle-mode chirped high-contrast metastructure VCSEL fo r 106 Gb/s PAM4 transmission," *Optica*, vol. 11, no. 11, pp. 1567 – 1574, 2024, DOI: <a href="https://doi.org/10.1364/OPTICA.539252">https://doi.org/10.1364/OPTICA.539252</a>
- [4] Mindaugas Juodénas, Erik Strandberg, Alexander Grabo wski, Johan Gustavsson, Hana Šípová-Jungová, Anders Larsson, Mikael Käll, "High-angle deflection of metagrati ng-integrated laser emission for high-contrast microscop y," Light: Science & Applications, vol. 12, article 251, 20 23, DOI: https://doi.org/10.1038/s41377-023-01286-0
- [5] Pei-Nan Ni, Pan Fu, Pei-Pei Chen, Chen Xu, Yi-Yang Xi e, Patrice Genevet, "Spin-decoupling of vertical-cavity su rface-emitting lasers with complete phase modulation usi ng on-chip integrated Jones matrix metasurfaces," *Natur e Communications*, vol. 13, article 7795, 2022, DOI: <a href="https://doi.org/10.1038/s41467-022-34977-0">https://doi.org/10.1038/s41467-022-34977-0</a>
- [6] Meng-Hsin Chen and Cheng-Yu Lee, "GaAs gradient me tasurface for vortex beam emission with high deflection angles," *Optics Express*, vol. 33, no. 1, pp. 933 – 943, 2 025, DOI: <a href="https://doi.org/10.1364/OE.546874">https://doi.org/10.1364/OE.546874</a>
- [7] Wen Dandan, and Kenneth B. Crozier. "Semiconductor I asers with integrated metasurfaces for direct output bea m modulation, enabled by innovative fabrication method s." *Nanophotonics*, vol. 12, no. 8, pp. 1443 1457, 202 3, DOI: <a href="https://doi.org/10.1515/nanoph-2022-0585">https://doi.org/10.1515/nanoph-2022-0585</a>